

LA-UR-79-2058

CONFIDENTIAL

TITLE: MIRROR QUALITY REQUIRED BY THE ANTARES LASER SYSTEM

MASTER

AUTHOR(S): William C. Sweatt

SUBMITTED TO: LASL Conference on Optics '79  
Los Alamos, NM  
May 23-25, 1979

University of California

By acceptance of this article, the publisher recognizes that the U.S. Government retains a nonexclusive, royalty-free license to publish or reproduce the published form of this contribution, or to allow others to do so, for U.S. Government purposes.

The Los Alamos Scientific Laboratory requests that the publisher identify this article as work performed under the auspices of the U.S. Department of Energy.



LOS ALAMOS SCIENTIFIC LABORATORY

Post Office Box 1663 Los Alamos, New Mexico 87545  
An Affirmative Action/Equal Opportunity Employer

## MIRROR QUALITY REQUIRED BY THE ANTARES LASER SYSTEM\*

W. C. Sweet  
University of California  
Los Alamos Scientific Laboratory  
Los Alamos, NM 87545

NOTICE  
This report was prepared as an account of work sponsored by the United States Government. Neither the United States nor the United States Department of Energy, nor any of their employees, nor any of their contractors, subcontractors, or their employees, makes any warranty, express or implied, or assumes any legal liability or responsibility for the accuracy, completeness or usefulness of any information, apparatus, product or process disclosed, or represents that its use would not infringe privately owned rights.

### Abstract

The Antares laser system is a large (100 kJ) CO<sub>2</sub> pulse laser operating at 10.6  $\mu\text{m}$ . The system has 72 beam lines, each with an aperture of 900 cm<sup>2</sup>. The system will be composed primarily of large copper-faced mirrors whose principal dimensions range up to 65 cm. These mirrors will be single-point diamond turned (SPDT) at the Y-12 facility of Union Carbide Corporation in Oak Ridge, Tennessee. We have had to develop surface quality specifications for these mirrors. These specifications were initially set at 50 nm peak-to-valley (p-v) surface error for the microsurface over 0.5-mm areas and 500 nm (p-v) over the whole mirror surface.

In this paper an attempt has been made to refine these specifications to a more physically meaningful set based on the performance of the system. The optical specification for Antares is that 80% of the energy from each beam should be deliverable inside a 400- $\mu\text{m}$  circle. The diffraction-limited focal spot is 160  $\mu\text{m}$  across, so small amounts of low spatial frequency wavefront aberrations are acceptable. This is the "figure error" and can be represented by a best-fit fourth-order polynomial. It is specified separately from the higher spatial frequency "subfigure" errors that diffract light out of the 400- $\mu\text{m}$  circle.

Antares will have a completely automatic alignment and centering system. A more versatile and less expensive alignment system can be developed if the alignment is done with visible light. This tightens the tolerances on the microsurface but not the figure error.

These requirements, along with several lesser ones, must be considered when tolerancing the mirror quality. It appears that the SPDT mirrors turned at Y-12 will meet our minimum requirements.

### Introduction

All of the large mirrors for the Antares laser system (Fig. 1) will be single-point diamond turned (SPDT) at the Y-12 facility of the Union Carbide Corporation in Oak Ridge, Tennessee. The trapezoidal-shaped spheres (40 cm by 30 cm) and flats (up to 65-cm diagonal) are to be cut to the following specifications; the peak-to-valley (p-v) surface microfinish shall be less than 50 nm over a 0.25-mm field, while the large scale surface contour errors visible on an interferogram should be less than 500 nm p-v.\* It is proposed that this set of requirements be modified and somewhat relaxed to a more physically meaningful set based on the amount of 10.6- $\mu\text{m}$  radiation diffracted out of the beam and also the scattering of a visible alignment beam.

The Antares optical specification is to deliver 80% of the light energy from each beam line into a 400- $\mu\text{m}$ -diameter circle. Thus, those errors that would diffract light out of the 400- $\mu\text{m}$  circle should be tolerated separately from those that don't. With moderate wavefront errors [ $w(x,y) \ll 10.6 \mu\text{m}$ ], as we should expect in Antares, this division can be made based on the spatial frequency contents of the surface errors.

To calculate the maximum spatial frequency that will not diffract light out of the 400- $\mu\text{m}$  circle, we proceed as follows: Assume the mirror surface has a sinusoidal variation across it  $w(x) = \cos 2\pi x/D$  where  $D$  is the inverse of the spatial frequency and  $\lambda$  is to be determined. A small ( $w \ll \lambda$ ) sinusoidal error like this will diffract some light into the plus and minus one orders as shown in Fig. 2. The 400- $\mu\text{m}$  circle is shown in Fig. 3. The plus and minus one orders can translate at 120  $\mu\text{m}$  and still remain in the 400- $\mu\text{m}$  circle. This will be true if  $D \geq 1.6 \text{ m} \times 10.6 \mu\text{m}/120 \mu\text{m} = 14 \text{ cm}$ .

The highest spatial frequency wavefront error that does not diffract light out of the 400- $\mu\text{m}$  circle is shown in Fig. 4. Note that sinusoidal terms up to this spatial frequency will, when summed appropriately, represent any fourth order polynomial.

\*Work performed under the auspices of the U.S. Department of Energy

Therefore, any third order wavefront errors (which are derived from fourth order wavefront errors, will not diffract a significant amount of light out of the 400- $\mu\text{m}$  circle, assuming  $w(x,y) \ll \lambda$ . The third order aberrations and the focus error will be defined as the "figure error" and shall be tolerated separately from the higher order errors that diffract light out of the 400- $\mu\text{m}$  circle.

To analyze a mirror then, defocus and third order aberration terms are fit to the interferometrically determined surface using least-squares (the computer code FRINGE  $\pm 1\%$  will do this). The residual error will be of higher frequency and will diffract light out of the 400- $\mu\text{m}$  circle. Its rms value must be tolerated separately. These errors shall be called the "subfigure error".

Another minor constraint on the machining is to keep light from retro-diffracting back into the gain region of the power amplifier. This would cause parasitic oscillations. It can easily be done by avoiding certain scan sequence rates as will be discussed at the end of this paper.

#### Diffrraction Theory

Only a small amount of the 10.6- $\mu\text{m}$  light can be permitted to be diffracted out of the beam if Antares is to deliver 90% into a 400- $\mu\text{m}$  circle, considering all of the possible problems that could sap energy from the beam. Thus, only small surface errors ( $w(x,y) \ll 10.6 \mu\text{m}$ ) can be allowed at each mirror. As a result, the Fourier theory of optics (diffraction theory,<sup>3</sup>) can be used for this analysis.

#### The Subfigure

The wavefront error  $w(x,y)$  is the sum of the various independent error sources. Included are the cusping due to the tool radius, the random tool motion, the local non-straightness of the ways, and slowly varying effects like temperature variations which affect the figure.

$$w(x,y) = w_{\text{cusp}} + w_{\text{random}} + w_{\text{ways}} + w_{\text{subfigure}} + w_{\text{figure}} \quad (1)$$

All of these errors, except the figure, vary quite rapidly over the mirror surface so each diffracts a small component of the light widely; that is, far outside the 400- $\mu\text{m}$  circle. As a result, the period of a 1" size is unimportant. The only parameter that affects the energy in the 400- $\mu\text{m}$  circle is the rms deviation from the best-fit (fourth order polynomial). The energy loss can be written as

$$\frac{E}{E_{\text{total}}} = \left( \frac{4\pi}{\lambda} \right)^2 (\text{rms})^2 = \left( \frac{4\pi}{\lambda} \right)^2 1/A \iint [w(x,y) - w_{\text{figure}}]^2 dA \quad (2)$$

If Eq. (1) is substituted into Eq. (2), then the integral is

$$\iint [w(x,y) - w_{\text{figure}}]^2 dA = \iint [w_{\text{cusp}} + w_{\text{random}} + w_{\text{ways}} + w_{\text{subfigure}}]^2 dA$$

These rapidly varying terms are all independent of one another so the cross-product terms in the integral are all zero. Thus, the energy diffracted out of the 400- $\mu\text{m}$  circle is the energy diffracted by the cusps added to the energy diffracted by the random tool motion plus that diffracted by the nonstraightness of the ways and the subfigure.

$$\frac{E}{E_{\text{total}}} = \left( \frac{4\pi}{\lambda} \right)^2 1/A \left( \iint w_{\text{cusp}}^2 dA + \iint w_{\text{random}}^2 dA + \iint w_{\text{ways}}^2 dA + \iint w_{\text{subfigure}}^2 dA \right)$$

Now replace the integrals with the rms surface variations, giving

$$\frac{E}{E_{\text{total}}} = \left( \frac{4\pi}{\lambda} \right)^2 \frac{2}{I} \text{total} \cos^2 I \quad (3)$$

$$\text{total}^2 = \text{cusp}^2 + \text{random}^2 + \text{ways}^2 + \text{subfigure}^2$$

where  $I$  is the angle of incidence of the beam on the mirror.

190-35

### Setting a Subfigure Roughness Specification

We hope to use visible light to center and align the beam through the system of mirrors in Antares. A visible alignment scheme would be less expensive, more versatile, more accurate for centering, and self-verifying. The price we pay for these benefits is a tighter tolerance on the mirror microfinish.

During the beam centering operation a telescope in the front end of the system will be focused on the mirror upon which the beam is being centered. Hence, the beam size upstream of said mirror will be at most 3 cm across, rather than nearly 30 cm as it is when the beam is focused on the target. Thus, only the center 3 cm of the large mirrors needs to have particularly high subfigure quality. Radiometric calculations show that these center portions should diffract 30% or less of a visible alignment beam. This means an rms figure error of 26 nm as per Eq. (3). The rest of the mirror surface of all mirrors should scatter no more than 50% of a 633-nm beam which allows a surface roughness of 40 nm rms. As shown in Eq. (3), the energy loss in the system is a function of the product of the actual surface errors and the cosine of the angle of incidence. Thus, the allowable errors are greater in the mirrors with a higher angle of incidence. These requirements are summarized in Table I along with the fraction of the light that would be undiffracted at normal incidence; that which would be useful while taking an interferogram. These mirrors will each diffract 0.22% of a 10.6  $\mu\text{m}$  out of the 400- $\mu\text{m}$ -diameter circle, so six mirrors will scatter 1.3% of the total energy.

The total rms error must be apportioned to the cusping due to the tool radius, the random tool motion, and the errors associated with the non-straightness of the ways in an rms fashion, as shown in Eq. (3).

Table II gives the relationship between the p-v errors and the rms errors,  $\zeta_{cusp}$ ,  $\zeta_{random}$ , and  $\zeta_{ways}$ . The random tool motion ( $\zeta_{random}$ ) was assumed to be Gaussian; that is, it was assumed to be continuously moving in and out in a random fashion. If the random motion is near zero for long stretches and then the tool chatters for a few turns, this would not be Gaussian random motion and so the approximate p-v equivalences given in Table II would not be valid. Also in Table II are examples of an acceptable allocation of the 26 nm and 40 nm rms total error. In the examples, p-v errors of 145 nm and 200 nm would be possible. Figure 5 graphically displays the inequalities:

$$\zeta_{total} = 26 \text{ nm} \leq \sqrt{\zeta_{cusp}^2 + \zeta_{random}^2 + \zeta_{ways}^2}$$

and

$$40 \text{ nm} \geq \sqrt{(\zeta_{cusp}^2 + \zeta_{random}^2 + \zeta_{ways}^2)}$$

TABLE I

Mirror	Angle of incidence	Allowable Overall Subfigure (rms)	Allowable Central Region Subfigure	633-nm Light Undiffracted at Normal incidence	Allowable Surface Figure Error (rms)
Back Reflector	0	40 nm	26 nm	50%	35 nm
Periscope 1	120	52 nm	29 nm	38%	55 nm
Periscope 2	120	52 nm	29 nm	48%	35 nm
Turning Chamber Mirrors	1450	57 nm	40 nm	20%	120 nm
Fold Flats	1270	44 nm	44 nm	43%	95 nm
Parabolas	00	40 nm	10 nm	50%	170 nm

150-35

TABLE II

Error	RMS/P-V	Examples (res/p-v)
Cusping	.30/1.	7.5 nm/25 nm 7.5 nm/25 nm
Random Tool Motion	.35/1.	17.5 nm/50 nm 25 nm/70 nm
Nonstraightness of Ways	.29/1.	19 nm/68 nm 29 nm/100 nm
Combined Effects		28 nm/143 nm 40 nm/195 nm

The Figure Error

Due to target physics considerations, the Strehl ratio<sup>4</sup> of the Antares system should be kept above 30%, which means 10% of the light energy can be lost out of the central core of the focused spot. Allowing a 1% loss for the microfinish and subfigure, the remaining 9% sets the tolerance on the figure error. From Eq. (2) the combined rms figure error can be calculated to be  $\sigma_{fig} = 250 \text{ nm}$ .

The figure error is a combination of the third order astigmatism, coma, and spherical aberration. Power on a tilted mirror produces astigmatism, also. Tolerancing these mirrors is very subjective at best. The mirrors with a large angle of incidence will be longer than they are wide by the arc-secant of the angle, making them more likely to show astigmatism when they are taken off the machine. But, in addition, the errors have a lesser effect proportional to the cosine of the angle. Power on these tilted mirrors is also a problem. The allowable rms error is somewhat arbitrarily chosen as  $\sigma = c$  for on-axis mirrors,  $\sigma_p = 2c$  for the off-axis parabola, and  $(\sigma_T = c/\cos I)$  for the tilted components. Taking the root of the sum of the square and setting it equal to 250 nm rms surface gives the rms figure errors in Table I.

In Table III the appropriate ratios of the rms aberrations to the peak-to-valley are given for the third-order aberrations. The rms values are calculated at the best focal positions while the p-v values represent the aberration at the Gaussian image plane. So, to calculate the figure error, the amounts of third-order aberrations can be calculated from interferogram data using FIGURE III.<sup>5</sup> The values can be multiplied by the coefficients in Table III, giving the rms figure error. The results can be compared with the allowable amounts in Table I.

TABLE III  
RATIO OF RMS VALUES OF THE BEST BALANCED ABERRATION  
TO THE PEAK-TO-VALLEY UNBALANCED ABERRATIONS

Aberration	Integral of Balanced Aberration	Variance	rms/p-v
Astigmatism	$1/A \int \int  x^2 - 1/2(x^2 + y^2) ^2 dA = .0444$		.21
Coma	$1/A \int \int [(x^2 + y^2)y - \frac{14}{15}y]^2 dA = .0525$		.23
Spherical	$1/A \int \int [(x^2 + y^2)^2 - 2/9(x^2 + y^2)]^2 dA = .00625$		.08
Power	$Ast (1/\cos I - \cos I)$	----	$.21(1/\cos I - \cos I)$

190-35

#### Measuring Macro and Micro Deviations From the Best-Fit Polynomial

The best-fit polynomial needed for this representation is of fourth order; a convenient choice because FRINGE III has Seidel aberrations with which a completely general fourth-order polynomial can be generated.

FRINGE III can also calculate the rms deviation from the polynomial if the interferogram is sampled fairly uniformly. This is called the subfigure error. The microroughness must include all errors whose period is too small to be seen on the interferogram. If, for example, errors of 2 mm period can barely be resolved on the interferogram, then the device used to measure the microroughness must have a field of view of at least 2 mm.

The subfigure and microroughness can be added in a root-sum-square fashion to give the total rms deviation of the surface from the best-fit polynomial.

$$\sigma_T = \sqrt{(\sigma_{\text{macro}}^2 + \sigma_{\text{micro}}^2)} . \quad (5)$$

#### Experimental Work

Y-12 had finished their prototype mirror cutting at the time this was written (June 1979) and were about to begin their first production run. Figure 6 is a 633-nm interferogram of one of the prototype SPOT surfaces. The figure appears to be about a half of a fringe peak-to-peak, so its rms value should be roughly  $633 \text{ nm} / (2 \times 2 \times 3)$ , approximately 50 nm. The subfigure appears to be less than 1/4 fringe so the rms is about 25 nm; both well within the tolerances proposed.

The microfinish of a "sister" sample was traced with a Taylor-Rank-Hobson Talley step machine (Fig. 7). Figure 8 shows a typical section of the trace along with a "best fit" line showing the deviation of the valleys. This is caused by the random tool motion. The errors are

$$\sigma_{\text{tool}} = 10 \text{ nm} \quad \text{and} \quad \sigma_{\text{random}} = 3 \text{ nm} .$$

This mirror microroughness should diffract 0.006% of the energy out of a 10.6-μm beam, not counting subfigure errors. The microroughness will also diffract 1.5% of a 633-nm alignment beam at normal incidence. This was roughly verified in that diffraction plus absorption attenuated a HeNe beam by 9%; 6-3% being absorption. Assuming no unforseen problems, the mirror quality is comfortably better than the minimum requirement.

#### Tool Advance Rates

The cutting tool is advanced at a uniform rate, giving a uniform spacing of the peak and valley. As such, the mirrors could act as a grating and diffract light back into the gain region, causing parasitic oscillations. The parasitic problem can be avoided if the mirrors near the gain region (the periscope mirrors) are cut such that the distance between peaks on the mirrors is not in the ranges

$$z = \frac{n\lambda}{2 \sin \theta}, \quad n = 1, 2, \dots$$

The Woods anomaly is an energy loss mechanism that could also cause us trouble. It can occur when the peaks are separated by an integral number of wavelengths, so avoid the spacings,  $z_w = 10.6 \mu\text{m}, 21.2 \mu\text{m}$ , etc.

#### Recommendations

It is proposed that the figure be specified separately from the subfigure and microfinish. The figure requirements are generated from a target physics point of view. All other errors should be added in an rms fashion and specified together since they represent the energy diffracted out of the 400-μm circle. These are all tabulated in Table I.

150-35

The errors can be determined if an interferogram is made of the whole part and if several microscopic interferograms are made of areas on the surface that are somewhat larger than the minimum resolvable error of the large interferogram. The large interferogram must be reduced using as uniform a grid as possible. For example; 15 nearly straight fringes, each of which is sampled every 15 nm, would be quite adequate. The reduction can be done using FRINGE III. The figure error can be removed with aberration coefficients through third order; the remainder being subfigure error that FRINGE III can easily remove. The microfinish error can be determined using a similar uniform sampling scheme. This error can be added in an rms fashion to the subfigure error to see if the mirror meets specifications which are listed in Table I (40 nm rms generally with tighter tolerance on the central regions of some mirrors).

The test pieces run thus far indicate an rms microfinish of 15 nm and the rms subfigure error should be less than 13 nm. These numbers are comfortably within the specifications so it appears that we should easily exceed our specification of 30% of the energy in a 400- $\mu\text{m}$ -diameter circle.

#### References

1. E. O. Swickard, Editor, "Antares Project Data Document" Los Alamos Scientific Laboratory, internal document.
2. John Loomis FRINGE User's Manual, Version III, November 1976, University of Arizona, Tucson, Arizona.
3. J. W. Goodman, Introduction to Fourier Optics, McGraw-Hill, 1968.
4. Born and Wolf, Principles of Optics, Pergamon Press, 1975.
5. Q. Appert Los Alamos Scientific Laboratory, personal communication, April 1973.

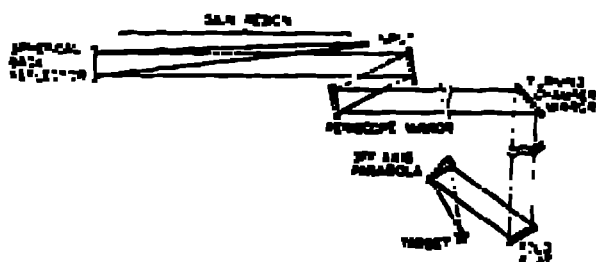


Fig. 1. Schematic of the large SPOT optics in one of the 72 Antares beam lines.

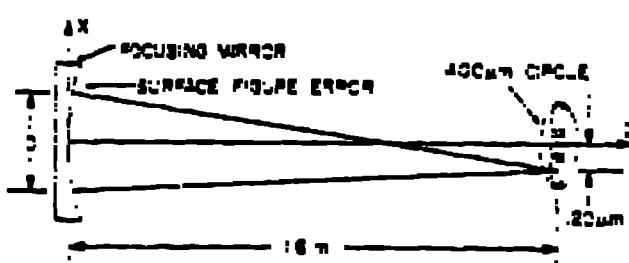


Fig. 2. A sinusoidal wavefront error on the mirror will diffract light into the first order.

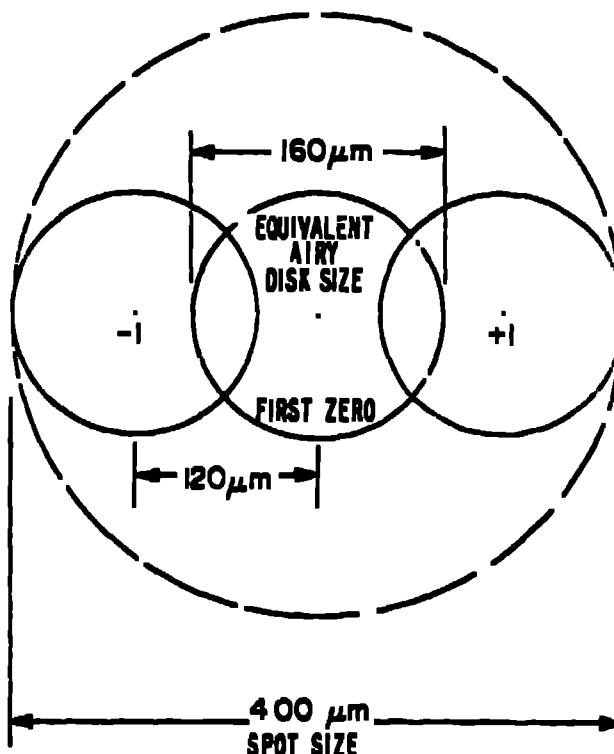


Fig. 3. A 400- $\mu\text{m}$  circle with first orders diffracted to the edge.

190-35

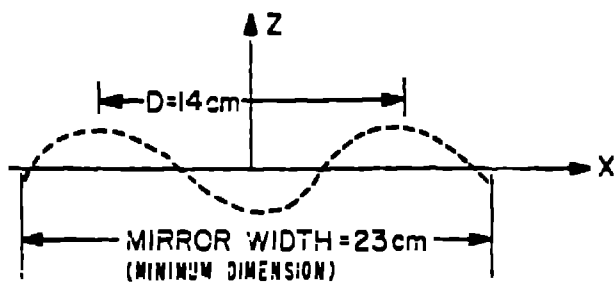


Fig. 4. Surface figure error with highest spatial frequency not diffracting light out of 400- $\mu$ m circle.

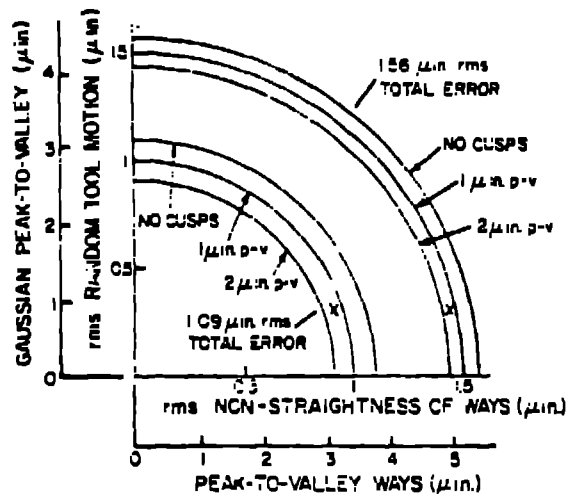
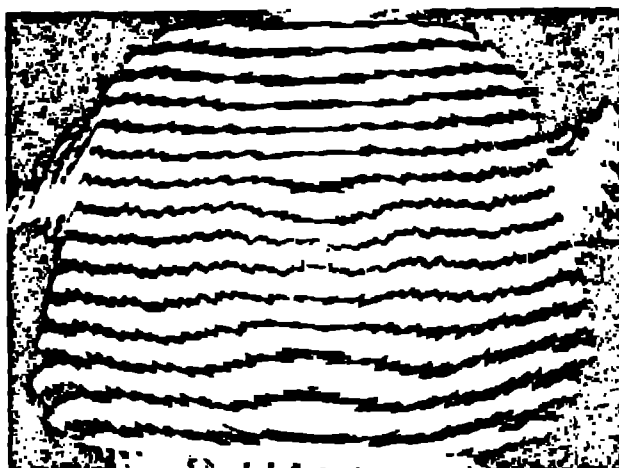


Fig. 5. Allowable peak-to-valley and rms tool motion and nonstraightness of ways for 1.49 and 1.56-in. rms error requirements.



INTERFEROGRAM OF RECENTLY CUT 33 x 33 cm SPOT FLAT MIRROR

Fig. 6. Interferogram of a prototype SPOT Antares mirror.



Fig. 7. Talley step trace of a prototype SPOT Antares mirror.